ISSN 1330–0008
CODEN FIZAE4

USE OF MAGNETIC SHEAR FOR THE IMPROVEMENT OF QUALITY OF CONFINEMENT IN THE PLASMA OF TOKAMAK

M. EL MOUDEN[a], D. SAIFAOUI[a,1], A. DEZAIRI[b] and H. IMZI[a]

[a]*Laboratory of Theoretical Physics, Faculty of Sciences - Ain Chock, Casablanca, Morocco*

[b]*Laboratory of the Physics of Condensed Matter, Faculty of Sciences - Ben M'sik, Casablanca, Morocco*

[1]*Corresponding author; E-mail address: dsaifaoui@caramail.com*

Received 21 July 2004; revised manuscript received 17 March 2005
Accepted 6 June 2005 Online 16 February 2006

We investigate the influence of reversed shear on the improvement of the confinement's quality in the plasma of a tokamak, specifically in reducing the anomalous transport. We use a special model for the drift wave fields. Comparison between the particle trajectories for normal and reversed shear is carried out in 2D and 3D presentation. The diffusion coefficient of particles and the radial electric field for the two cases, normal and negative shear, have been evaluated.

PACS numbers: 52.55.Fa, 52.55.Dy, 52.25.Fi UDC 533.95, 533.93

Keywords: plasma confinement, tokamak, anomalous transport, magnetic shear, transport barrier, particle diffusion, radial electric field, enhanced confinement

1. *Introduction*

In recent years, the study of the anomalous transport in the plasmas of tokamaks has become the focus of research as it is claimed it serves to control thermonuclear fusion. It is very well known that the destruction of magnetic surfaces, which are responsible for the plasma confinement, the stochastic region's formation, the anomalous transport of particles and energy, etc., resulting in magnetohydrodynamic instabilities, electrostatic and magnetic turbulence and the phenomena of drift, cause the deterioration of the confinement. Concerning this fact, all effort in this sense requires the understanding of the origin of this transport, of the instabilities that exist in the plasmas of the tokamaks and the development of reliable theoretical models that are capable of describing the complex dynamics of fusion plasma [3,5 – 9].

The aim of this study is to survey the dynamics of the lines of magnetic fields, and of plasma particles in the ulterior stage and to study the contribution of the reversed shear to the improvement of the plasma confinement in tokamaks, and also other rules of improvement of the confinement. Indeed, the research concentrates currently more on the control of these improved confinement régimes that have been observed during the last decade. These are the régimes where we observe reduction of the plasma diffusion, and what is impressive is the formation of the transport barrier. We use the word "barrier" because it opposes the anomalous diffusion of particles, taking the shape of an obstacle to particles of plasma. We studied the motion of the guiding center of particles, under the action of electrostatic field perturbation, in a configuration known as the reversed magnetic shear. This configuration is adopted more and more in the new machines of fusion, since it leads to important reductions in the diffusion coefficients. The equations of motion of the guiding center will be replaced by equations of mapping known as the nontwist standard mapping, and, in the phase space of the particles, we simulate the trajectory in two completely different cases of the safety factor profile: the normal profile and the reversed one. In the normal case, the trajectory can be described by the KAM theory, while in the reversed case, the dynamics is described by the formation of the transport barrier of the particles that are localized in the neighborhood of the resonance surface that corresponds to the minimum of q. This surface confines plasma and reduces its diffusion.

2. Mapping equations

2.1. Equation of motion

In our survey, we use a simplified model of an equilibrium magnetic field, according to a toroidal geometry, which is described by the following relation [12 – 16]

$$\vec{B} = B_\theta(r)\vec{e}_\theta + B_\varphi \vec{e}_\varphi \, , \tag{1}$$

which consists of the poloidal magnetic field component and the toroidal magnetic-field component which are bound by the relation $B_\theta(r) = rB_\varphi/(q(r)R_0)$, of which r is the minor radius of plasma, θ and φ are respectively the poloidal and toroidal angle, and finally, $q(r)$ is the safety factor. In the Gaussian system of units, the equation of motion of the guiding center is given by

$$\frac{\mathrm{d}\vec{x}}{\mathrm{d}t} = v_{||} \, \frac{\vec{B}}{||\vec{B}||} + c\frac{\vec{E} \wedge \vec{B}}{B^2} \, , \tag{2}$$

where, $v_{||}$ is the parallel velocity, $\vec{E}$ and $\vec{B}$ are the electric and magnetic fields, and the last term of this equation represents the drift velocity. The electric field satisfies the relation

$$\vec{E} = -\vec{\nabla}\phi\,. \tag{3}$$

The corresponding electrostatic potential, ϕ, can be written as a sum of two terms, the first is the radial part supposed to be in equilibrium, and the second one represents the fluctuating part, noted $\tilde{\phi}$. We use the model of the spectrum of drift wave, and we have

$$\tilde{\phi} = \sum_{m,l,n} \phi_{m,l,n} \cos(m\theta - l\varphi - n\omega_0 t)\,, \tag{4}$$

where ω_0 is the lowest angular frequency in the spectrum of drift wave, and θ and φ are random variables. The disrupted electrostatic field $\tilde{E}$ is related to the potential of perturbation by [10] $\tilde{E} = -\vec{\nabla}\tilde{\phi}$. In the continuation of our survey, we suppose that $B \approx B_\varphi \gg B_\theta$ and $B_r = 0$ in the system of toroidal coordinates (r, θ, φ), and we introduce $\bar{E}_r$ as the equilibrium radial electric field. The previous equation of motion in this system of coordinates leads to the following system of equations

$$\begin{aligned} \frac{\mathrm{d}r}{\mathrm{d}t} &= -\frac{c}{B}\frac{1}{r}\frac{\partial\tilde{\phi}}{\partial\theta}, \\ r\frac{\mathrm{d}\theta}{\mathrm{d}t} &= v_{||}\frac{B_\theta}{B} + \frac{c}{B}\frac{\partial\tilde{\phi}}{\partial r} - \frac{c\tilde{E}_r}{B}, \\ R\frac{\mathrm{d}\varphi}{\mathrm{d}t} &= v_{||}\,. \end{aligned} \tag{5}$$

Substituting (4) into (5), we obtain

$$\frac{\mathrm{d}r}{\mathrm{d}t} = -\frac{c}{Br}\frac{\partial}{\partial\theta}\sum_{m,l,n}\phi_{m,l}\big[\cos(m\theta - l\varphi)\cos(n\omega_0 t) + \sin(m\theta - l\varphi)\sin(n\omega_0 t)\big]. \tag{6}$$

Using the following two important properties of functions sin and cos,

$$\sum_{n=-\infty}^{\infty}\sin(n\omega_0 t) = 0 \quad \text{and} \quad \sum_{n=-\infty}^{\infty}\cos(n\omega_0 t) = 2\pi\sum\delta(\omega_0 t - 2\pi n)\,,$$

we have

$$\frac{\mathrm{d}r}{\mathrm{d}t} = \frac{2\pi c}{Br}\sum_{m,l} m\phi_{m,l}\sin(m\theta - l\varphi)\delta(\omega_0 t - 2\pi n)\,. \tag{7}$$

Hence, this model spectrum gives impulsive jumps in r at times $t_n = 2\pi n/\omega_0$.

2.2. Transformation into a mapping equation

It is advantageous to replace the equations of the guiding center particle motion by those of the mapping approach. To achieve that, we introduce new canonical variables. We define the new angle-action variables (χ, J) as

$$J = \left(\frac{r}{a}\right)^2 \quad \text{and} \quad \chi = M\theta - L\varphi\,. \tag{8}$$

a is the minor radius of the torus. Also, we suppose that only one perturbation mode (M, L) dominates in the equation of evolution of r.

From Eq. (7) we have

$$\frac{\mathrm{d}J}{\mathrm{d}t} = \frac{2r}{a^2}\frac{\mathrm{d}r}{\mathrm{d}t} = \frac{4\pi c}{a^2 B} M\phi_{m,l}\sin(M\theta - L\varphi)\sum_n \delta(\omega_0 t - 2\pi n)\,. \tag{9}$$

By integration over one jump at time $t_n = 2\pi n/\omega_0$, in terms of χ Eq. (5) becomes

$$\frac{\mathrm{d}\chi}{\mathrm{d}t} = M\frac{B_\theta}{rB}\left(v_{||} - \frac{c\bar{E}_r}{B_\theta}\right) - L\frac{v_{||}}{R}. \tag{10}$$

Ignoring in the first approximation of $\bar{E}_r$ the integration of the χ and J differential equations as the functions of time, we get their evolution equations

$$J_{N+1} = J_N + \frac{4\pi c}{a^2 B_0}\frac{M\phi}{\omega_0}\sin(M\theta - L\varphi)\,, \tag{11}$$

$$\chi_{N+1} = \chi_N + \frac{2\pi}{\omega_0}\frac{v_{||}}{qR}(M - Lq)\,. \tag{12}$$

2.3. The standard nontwist mapping (SNM)

The important parameter which allows us to construct this model is the safety factor replaced here for convenience by $q(r) = rB_\varphi/(RB_\theta)$. We suppose that this safety factor has a local minimum in the neighbourhood of a certain value r_m, meaning that $q_m = q(r_m)$, $q'(r_m) = 0$, since

$$\left.\frac{\mathrm{d}q}{\mathrm{d}J}\right|_{r=r_m} = \left.\frac{\mathrm{d}q}{\mathrm{d}r}\right|_{r=r_m} \times \left.\frac{\mathrm{d}r}{\mathrm{d}J}\right|_{r=r_m} = 0\,.$$

Then q possesses a minimum at $J_m = J(r_m)$. We are interested in the motion of particles in the neighbourhood of r_m, and we do a Taylor expansion of q around J_m, that we can write as

$$q(J) = q(J_m) + \frac{q''_m}{2}(J - J_m)^2.$$

Substituting the last equation into Eq. (10), we get

$$\frac{\mathrm{d}\chi}{\mathrm{d}t} = \frac{v_{||}}{Rq_m}\left[M - Lq_m - \frac{Mq''_m}{2q_m}(J - J_m)^2\right], \tag{13}$$

and after integration over the step of time $1/(\Delta\omega)$, we obtain

$$\chi_{N+1} = \chi_N + \frac{2\pi}{\omega_0}\frac{v_{||}}{Rq_m}\left[\delta - \frac{Mq''_m}{2q_m}(J_{N+1} - J_m)^2\right], \tag{14}$$

where $\delta = M - Lq_m$. We introduce the dimensionless variables K and T such that

$$K = \frac{\chi}{2\pi} \quad \text{and} \quad T = \sqrt{\frac{Mq''_m}{2q_m\delta}}(J - J_m) = k(J - J_m)\,.$$

Hence, we can transform the system of mapping equations to the SNM form

$$K_{N+1} = K_N + \frac{v_{||}\delta}{Rq_m\omega_0}(1 - T^2_{N+1}) = \chi_N + \alpha(1 - T^2_{N+1})\,, \tag{15}$$

$$T_{N+1} = T_N + \frac{2\pi cM\phi}{a^2B\omega_0}\sqrt{\frac{2Mq''_m}{q_m\delta}}\sin(2\pi K_N) = T_N - \beta\sin(2\pi K_N)\,, \tag{16}$$

where

$$\alpha = \frac{v_{||}\delta}{Rq_m\omega_0} \quad \text{and} \quad \beta = \frac{-2\pi cM\phi}{a^2B\omega_0}\sqrt{\frac{2Mq''_m}{q_m\delta}}\,.$$

2.4. *Global Mapping*

In order to introduce the effects of the reversed magnetic shear and of the radial electric field, we define the system of equations of global mapping as follows [7,10–16]

$$J_{N+1} = J_N + \frac{4\pi c}{a^2B_0}\frac{M\phi}{\omega_0}\sin(M\theta_N - L\varphi_N)\,, \tag{17}$$

$$K_{N+1} = K_N + RK_1(J_{N+1}) + RK_2(J_{N+1})\,, \tag{18}$$

where

$$RK_1(J) = \frac{v_{||}(J)}{\omega_0 qR}(M - Lq(J))\,, \tag{19}$$

$$RK_2(J) = -\frac{cM}{\omega_0 aB_0}\frac{\bar{E}_r(J)}{\sqrt{J}}\,, \tag{20}$$

$$v_{||}(J) = \sqrt{\frac{2}{m}(\zeta_t - e\Phi_0(J))(1 - \lambda B_0)}\,, \tag{21}$$

where $K = \chi/(2\pi)$, ζ_t is the total initial energy, e is the particle charge and $\lambda = \mu/\zeta_t$, where μ is the magnetic moment and Φ_0 is the equilibrium potential given by

$$\bar{E}_r(J) = -\frac{\partial \Phi_0}{\partial r}\bigg|_{r=a\sqrt{J}} .$$

Choice of the profiles of the factor of security

The trajectories have been solved numerically according to this formulation of established mapping. However, we are going to give more importance to the control parameter q, and we are going to consider two configuration cases that are completely different. We define two q-profiles (see Fig. 1.):

$$\wp \quad \text{Normal:} \qquad q(r) = 1.99 + 1.94\left(\frac{r}{a}\right)^2, \tag{22}$$

$$\wp \quad \text{Reserved:} \qquad q(r) = 1.99 + 7.76\left(\frac{r}{a} - 0.5\right)^2. \tag{23}$$

The choice of the potential Φ_0 depends on the nature of the q-profile, therefore, in the normal case we use $\Phi_0(r) = -\Phi_0(1 - (r/a)^2)$ and for the reversed profile we take $\Phi_0(r) = \Phi_0(1 - (1 - 2r/a)^2)$.

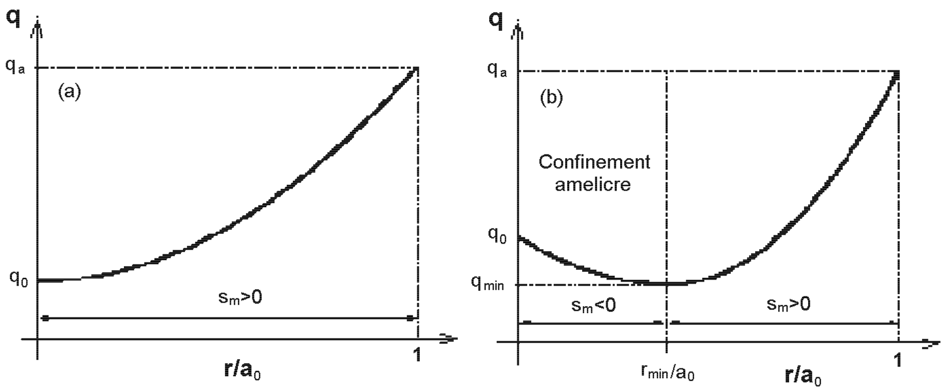

Fig. 1. Profile of the safety factor versus r/a for reversed (right hand) and normal (left hand) shear.

3. Numerical integration and interpretations

In the next section, we neglect the electric field radial component and investigate the map phase structure by calculating 1000 massive D^+ trajectories with various initial conditions in configuration space for the reversed and normal shear cases of the safety factor. In the calculation below, we have used the Texas Experimental Tokamak (TEXT) system parameters, with major radius $R_0 = 100$ cm, minor radius $a = 26$ cm and center-line field $B = 3$ T. We took $\omega_0 = 1.93 \times 10^5$, and we chose the mode of perturbation ($M = 12$, $L = 6$) and $\lambda = \mu/\zeta$, with $\zeta = 167$ eV, the energy of the particles.

Simulations and interpretations

In the presence of the electrostatic perturbations and the normal profile of the safety coefficient q, the stochasticity of the trajectories increases and it is the primary reason for the particles' diffusion through the magnetic surfaces (Fig. 2b). However, in the case of the reversed shear, the principal result shows that there exists a transport barrier near the surface that corresponds to the minimal value of q. This barrier plays an important role in the reduction of the transport and the diffusion of particles, and results in the improvement of the plasma confinement (Fig. 2a). In the case of the 3-dimensional simulation, we observe the same phenomena as those in the case of 2-dimensional simulation, except that we do not see the formation of islands, and what we observe is a transition of particles from the regions $r/a < 0.5$ toward regions $r/a > 0.5$.

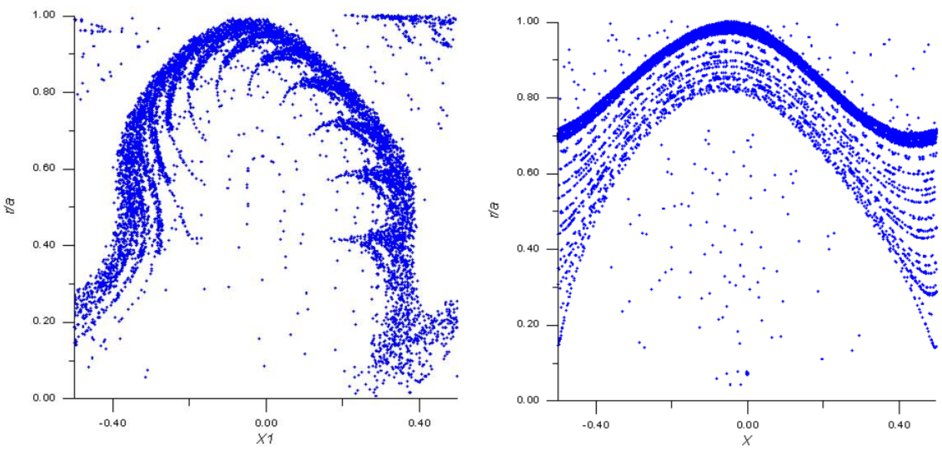

Fig. 2. Poincaré section for 1000 particles in the $(\chi, r/a)$ plane for the value 1.5 eV *of the perturbation: (a) reversed shear; (b) normal shear.*

When increasing the amplitude of the perturbation, and in the reversed case (Fig. 3a), we observe that this change drives the barrier toward the outside regions of the tokamak ($r/a \to 1$) to prevent the diffusion of particles. But in the normal case (Fig. 3b), we observe that the majority of particles escaped resulting in a total destruction of the magnetic surfaces of confinement.

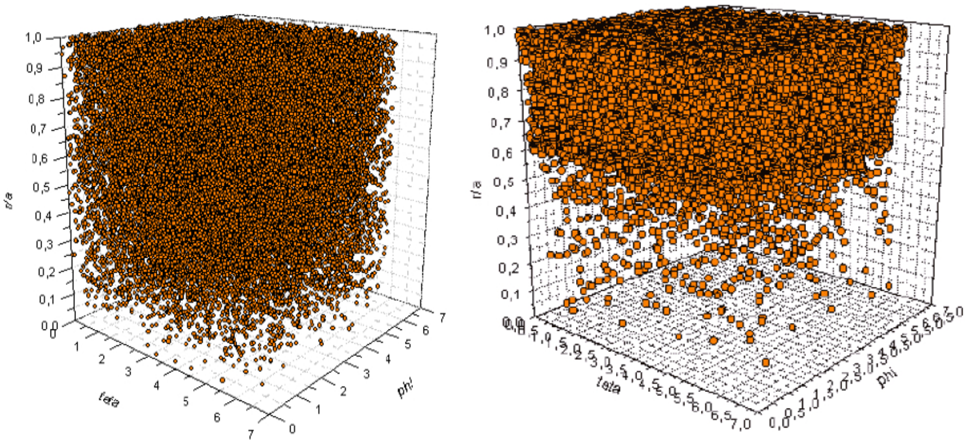

Fig. 3. 3-dimensional simulation of trajectories of 1000 particles at $(\theta, \varphi, r/a)$ for the perturbation of 1.1 eV*: (a) reversed shear, (b) normal shear.*

4. Diffusion of particles

To evaluate the plasma particles' diffusion through the magnetic surfaces within the tokamak reactors, we simulated in two cases the diffusion coefficients. We expressed them by the classic formula as follows [12 – 16]

$$D = \lim_{N \to \infty} \frac{\langle (r_N - r_0)^2 \rangle}{2t_N} \tag{24}$$

and we represented time evolution of the ratio of the reversed-shear diffusion coefficient (D_r) to the diffusion coefficient in the normal case (D_n) for different values of the perturbation (Fig. 4). t_n is the time step. We observe a large reduction of

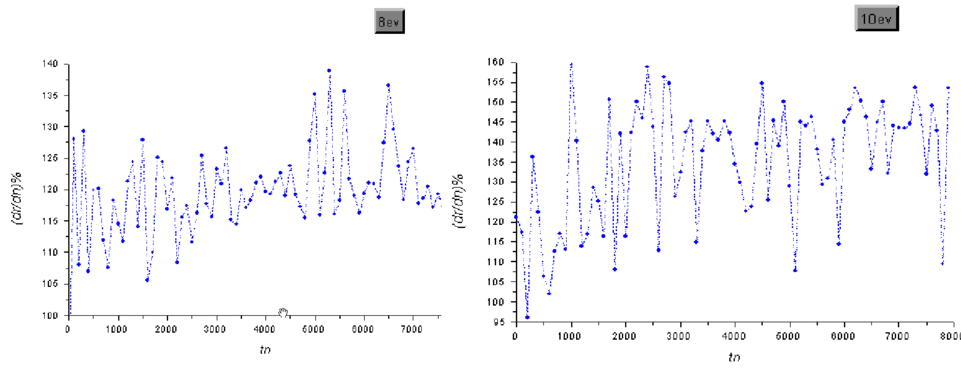

Fig. 4. The ratio between the diffusion coefficient in reversed and normal shear as function of t_n.

particle diffusion in the reversed case due to the transport barrier which tends to suppress the anomalous transport. The diffusion in the reversed case is lower than in the normal case. The formation of the transport barrier which suppresses turbulent transport may explain this reduction [4]. Finally, we represented the same ratio but now as a function of the amplitude of perturbation for different values of t_n (Fig. 5).

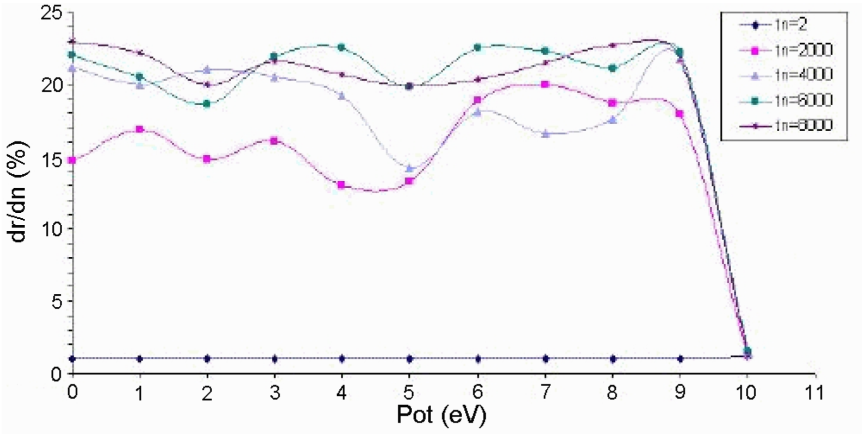

Fig. 5. The ratio between the diffusion coefficient in reversed and normal shear as function of the amplitude of perturbation.

5. *Radial electric field*

Effect of magnetic shear, heating power and applied torque on ITB formation [13]

Internal transport barriers (ITBs) have been identified in previous JET experiments from discontinuities in the gradients of the ion and electron temperatures as well as the plasma density and toroidal rotation velocity. Such discontinuities can be interpreted in terms of a local reduction in the energy, and particle and momentum transport. In the cases where the q-profile is monotonic, ITBs have generally been observed to form near integer q magnetic surfaces. A mechanism has been proposed to explain the link between ITB formation and rational q surfaces based on a local enhancement to the plasma flow shear due to the coupling of core and edge magnetohydrodynamic (MHD) modes. The power required to generate such a transport barrier at the $q = 2$ surface, where the most extensive database has been established, was seen to increase with toroidal magnetic field strength (or plasma current, which has the same dependence). The ITB access power for JET (in MW) scaled roughly as 5BT. Initial ITB experiments on plasmas with a region of negative magnetic shear in the core showed that ITBs could be obtained at much lower power levels. In this scenario, barriers were generated in the nega-

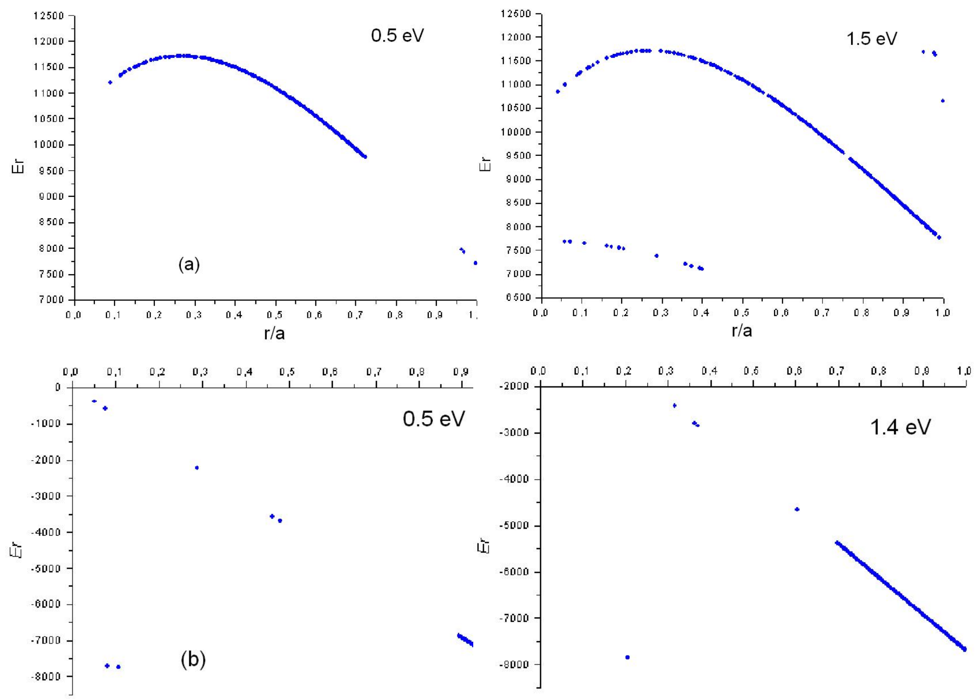

Fig. 6. Radial electric field as function of r/a for the value 0.5 eV *and 1.5* eV *of the perturbation: (a) reversed shear, (b) normal shear.*

tive magnetic shear region at a location that did not appear to be related to the location of a particular q surface and even during the preheating phase with very low levels of predominantly electron heating. It was possible to obtain both types of ITB simultaneously during high power heating, but at different plasma radii. In the experiments described in the previous section, a wide range of ITB phenomena have been observed. "Narrow" ITBs can be seen on the electron temperature profile during the low power lower hybrid current drive (LHCD) prelude phase in the case of "strongly" negative magnetic shear. These are discussed more fully elsewhere. In this paper, the term "narrow" is used to describe ITBs located close to the plasma centre (i.e. entirely within $r/a < 0.5$) as distinct from a small region of reduced transport (i.e. with $\Delta r_{ITB} \ll a$) located at large plasma radius. The core electron ITB can persist during the main heating phase depending on the parameters and timing of the main heating pulse. Even in the monotonic q-profile cases, "narrow" ITBs are sometimes seen on the ion temperature profile during the main heating pulse depending on the location of low order rational flux surfaces. These have also been generated at power levels much lower than 5BT and illustrate that this power scaling, obtained from a database of similar ITBs associated with $q = 2$, is not universally applicable to JET ITB formation even in cases with Ohmic preheating. This is thought to be due to a sensitivity to local conditions, such as the magnetic shear and the presence of MHD instabilities, and it is therefore concluded that a power threshold scaling based on global parameters alone is unlikely to adequately describe the complete ITB phenomenology. However, these "narrow" ITBs obtained at low heating power levels do not strongly improve the global plasma performance in terms of total stored energy or fusion yield. At higher main heating power levels, approaching 5BT, ITBs were obtained in these experiments at wider radius ($r/a < 0.6$) in both the LHCD and Ohmic preheat cases. These ITBs, seen on both the ion and electron temperature profiles, were able to provide a significant global plasma performance enhancement.

To intoduce the radial electric field, in the normal case, we use the same shape of the potential as before, but for the reversed one, we introduce a new expression which was used previously by Horton ($\Phi_0(r) = -\Phi_0(1-(r/a)^2)\exp\{1-r/a\}$) (see Fig. 6).

In the neighbourhood of the plasma border, the radial electric field E_r decreases, what causes a reduction of the potential electrostatic F_r, thereafter the reduction of the flight of the plasma ions and therefore the reduction of the anomalous transport with the shear.

6. *Conclusion and perspectives*

Anomalous transport observed in tokamaks is due to the electrostatic and magnetic turbulence. Thus, in the presence of electric perturbation and for the normal profile of the safety factor q, the stochasticity of the trajectories increases and this is the principal cause of diffusion of particles through magnetic surfaces. However, for the reversed shear case, the most important result is the impressive formation of a strong transport barrier, which is localized near the minimum value of q (q is the safety factor) (Fig. 2a). This barrier plays a very important role in the improvement of the plasma confinement while preventing its radial diffusion. To evaluate quantitatively the diffusion, we simulated from the Mapping equations, the diffusion coefficient in each of the two previous cases, and we drew the ratio that shows a clean reduction in the diffusion observed in the reversed magnetic shear profile. Therefore, the diffusion decreases, the confinement improves and the control of the fusion reactors to function in these modes permits the reduction of the anomalous transport in the tokamaks.

Lately, there has been consensus on an international scale to construct a big experimental reactor in Cadarache, International Thermonuclear Experimental Reactor (ITER). In this project, Europe, the USA, Canada, Australia, Japan and China will participate. The launch of this project in France is going to be a big step in the success of thermonuclear energy production. In this setting, and in perspective, we are going to reproduce the same simulations with the parameters of ITER to be able to compare them with those obtained for TEXT.

References

[1] S. B. Korsholm et al., *27th EPS Conf. Plasma Physics Cont. Fusion*, Budapest, Hungary (2000).

[2] T. D. Rogulien et al., Plasma Phys. Cont. Fusion **42** (2000) A271.

[3] V. Antoni et al., Plasma Phys. Cont. Fusion **42** (2000) A271.

[4] H. Takenaga et al., *Determination of Particle Transport Coefficients in Reversed Shear Plasma of JT-60U*, Plasma Phys. Control. Fusion **40** (1998) 183.

[5] B. Jhowry, Plasma Phys. Cont. Fusion **42** (2000) 1259.

[6] Y. Kamada, Plasma Phys. Cont. Fusion **42** (2000) A65.

[7] J. L. V. Lewandowski and M. Persson, Plasma Phys. Cont. Fusion **37** (1995).

[8] R. Tabet, D. Saifaoui, A. Dezairi and A. Rouak, Eur. Phys. J. AP. **4** (1998) 329.

[9] A. Oualyoudine, D. Saifaoui, A. Dezairi and A. Rouak, J. Phys. **7** (1997) 1045.

[10] Horton et al., *Drift Test Transport in Reversed Shear Profile* (August 1998).

[11] O. Fisher, W. A. Cooper and L. Villard, Nucl. Fusion **40** (2000) 1453.

[12] Horton et al., *Drift Wave Test Particle Transport in Reversed Shear Profile*, Phys. Plasmas **5** (1998) 3910.

[13] T. P. Kiviniemi, T. Kurki-Suonio and S. K. Sipila, Czech. J. Physics **49** (1999) S3.

[14] H. Imzi, D. Saifaoui, A. Dezairi and F. Miskane, Eur. Phys. J. AP. 17 (2002) 45.

[15] D. Saifaoui, *28th EPS Conf. Cont. Fusion Plasma Physics*, Madeira, Portugal (2001).

[16] F. Miskane, A. Dezairi, D. Saifaoui, H. Imzi, H. Imrane and M. Benharraf, Eur. Phys. J. AP. **13** (2001) 205.

UPORABA MAGNETSKOG SMIKA ZA POBOLJŠANJE ZADRŽAVANJA PLAZME U TOKOMAKU

Proučavamo utjecaj obrnutog smika za poboljšanje zadržavanja plazme u tokomaku, posebice za smanjenje anomalnog prijenosa. Primijenili smo poseban model za posmična valna polja. Usporedbu putanja čestica za normalan i obrnuti posmik načinili smo u 2D i 3D prostoru. Također smo odredili difuzijske koeficijente za čestice i radijalno električno polje za dva slučaja, normalan i obrnuti posmik.